Ultrafast Charge-Transfer Dynamics: Studies of *p*-Nitroaniline in Water and Dioxane

C. L. Thomsen, J. Thøgersen, and S. R. Keiding*

Department of Chemistry, University of Aarhus, Langelandsgade 140, DK-8000 Aarhus C, Denmark

Received: July 30, 1997; In Final Form: December 10, 1997

The intersystem crossing, internal conversion, and vibrational relaxation of *p*-nitroanaline (PNA) in water and 1,4-dioxane have been studied using ultrafast transient absorption spectroscopy. Following the photoexcitation of PNA at 400 nm, the transient absorption dynamics were probed from 340 to 960 nm. The measurements were performed on a common, absolute absorption scale, permitting an accurate determination of the temporal evolution of the absorption spectrum. The data reveal that relaxation on the excited singlet state surface, followed by internal conversion to the ground state and intersystem crossing to the triplet state, is extremely rapid (<0.3 ps) in both solvents. The observed intersystem crossing efficiency is $\Phi_{isc} \approx 0.4$ in dioxane and $\Phi_{isc} \approx 0.03$ in water, indicating that the coupling between the excited singlet and triplet states depends strongly on the solvent polarity. With the estimated quantum yield for intersystem crossing in water and dioxane, we find a time constant for intersystem crossing of ≤10 ps in water and ≤0.8 ps in dioxane. The transient absorption features observed in the visible region are assigned to vibrationally excited PNA in the electronic ground state and three triplet−triplet absorption bands.

I. Introduction

Disubstituted benzenes and, in particular, *p*-Nitroaniline (PNA) have served as important model molecules for theoretical[1−17] and experimental investigations[18−28] of charge-transfer properties. The simple structure of *p*-nitroanaline (PNA), with a donor group ($-NH_2$) linked via a phenyl ring to a strong acceptor group ($-NO_2$), makes PNA an interesting model system for studying intramolecular charge-transfer (CT) reactions and a variety of photophysical properties associated with the CT states. As shown in Figure 1, photoexcitation initiates the migration of charge from the amino group to the nitro group, leading to a change in the dipole moment of $\Delta\mu = 9.31$ D,[6] which corresponds to a charge transfer from the donating amino group to the accepting nitro group of 0.4 *e*. The large change in the dipole moment of PNA upon photoexcitation makes the intramolecular properties of PNA very susceptible to the dielectric response of the surrounding solvent. Thus, a 5000 cm^{-1} solvatochromatic shift of the CT absorption band of PNA has been observed when going from nonpolar to polar solvents.[21] Due to the relatively small energy difference between the lower excited states of PNA,[17] the strong energy dependence on the solvent polarity may in fact cause a change in the ordering of the lowest states.

The photophysics of PNA has been extensively studied using a variety of optical detection techniques.[6,13,18−28] A common feature found in these studies is a very short excited-state lifetime and the absence of any measurable fluorescence, indicating that deactivation proceeds entirely by very fast nonradiative processes such as intersystem crossing (ISC) and internal conversion (IC) to the electronic ground state (see Figure 1). Time-resolved microwave conductivity measurements[18] suggest that the quantum yield for intersystem crossing of PNA in benzene is close to 100%, whereas a reduced quantum yield of about 50% is observed for PNA in the slightly more polar dioxane, indicating that even small changes in the solvent polarity have a big impact on the quantum yield. This suggests that dissolving PNA in a very polar solvent, such as water, may result in a very small quantum yield.

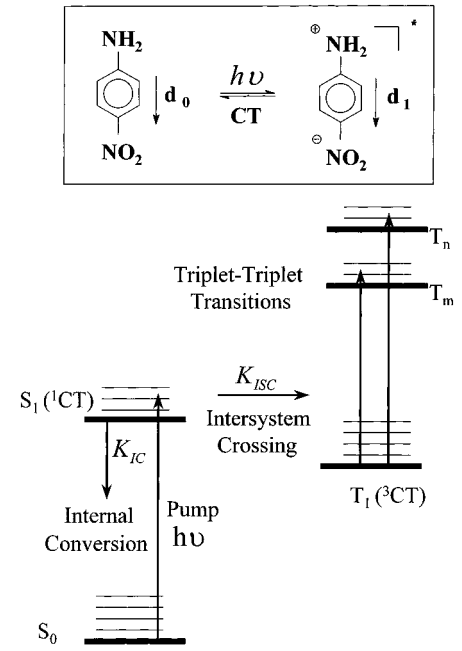

Figure 1. Photoexcitation initiates the migration of charge from the amino group to the nitro group, leading to a change in the dipole moment of $\Delta\mu = 9.31$ D, which corresponds to a charge transfer from the donating amino group to the accepting nitro group of 0.4 *e*. Following the optical preparation of the charge-transfer state by excitation within the charge-transfer absorption band, PNA undergoes a rapid intersystem crossing (ISC) to the triplet state or internal conversion (IC) to the ground state.

In this paper we study the intersystem crossing and internal conversion of PNA in water and dioxane by ultrafast transient absorption spectroscopy. Transient absorption induced by the excitation of PNA is measured at 20 wavelengths ranging from

* Corresponding author. E-mail: Keiding@kemi.aau.dk.

S1089-5639(97)02492-4 CCC: $15.00
Published on Web 01/23/1998

340 to 960 nm with a 300 fs resolution. By careful calibrations, the measurements are converted to a common scale in order to allow a quantitative comparison with previously obtained experimental as well as theoretical results.

The rest of this paper is organized as follows. After a brief description of the electronic structure of PNA in section II, the experimental setup is described in section III, and the experimental data of the pump−probe measurements on PNA in water and dioxane are presented in section IV. Then follows a discussion of the experimental data in section V, and finally, the paper is summarized in section VI.

II. Electronic Structure of PNA

The conceptually simple structure of PNA, with a strong donor and acceptor pair linked by an aromatic ring, has inspired a number of semiempirical calculations of the electronic structure.[14−17,20,22,25] In view of the present experiments, the most interesting calculation is the study of the triplet states by Bigelow et al.[17] using the semiempirical CNDO/S-CI method. From the work by Bigelow et al. we obtain the triplet electronic energy level diagram and the oscillator strengths for triplet−triplet transitions for gaseous PNA. However, it must be emphasized that a careful evaluation of the many theoretical calculations of the electronic structure in PNA shows very little agreement concerning the energy levels and the electronic structure of the excited states. In general, there is consensus among the different theoretical calculations that the charge-transfer state is a $^1\pi\pi^*$ transition, corresponding to transfer of charge from the amino group to the nitro group. Likewise, the lowest triplet state of PNA is in most cases the triplet counterpart to the charge-transfer singlet excitation, i.e., $^3\pi\pi^*$. However, the electronic energy level diagram for gaseous PNA should be used with caution in polar solvents, since some of the electronic transitions involve charge transfer and therefore depend on the solvent polarity, i.e., the singlet charge-transfer transition shifts more than 5000 cm^{-1} when going from nonpolar to very polar solvents.[21] Increasing the solvent polarity may lower the more polar $\pi\pi^*$ states relative to $n\pi^*$ with the possibility of causing an inversion of the states S_1 and T_1, since the general conclusion is that all of the lowest $\pi\pi^*$ and $n\pi^*$ singlet and triplet states of PNA are very close to each other.

III. Experimental Setup

The experimental setup is shown schematically in Figure 2. A regeneratively amplified titanium:sapphire laser from Clark-MXR with a repetition rate of 1 kHz was employed in this work. The output from the amplifier was 90 fs pulses with a wavelength centered at 800 nm and a pulse energy of 0.7 mJ. The fundamental beam was frequency doubled in a 0.2 mm BBO crystal to give the 400 nm pump pulse used to excite the PNA solution. A dichroic beam splitter separated the second harmonic from the fundamental beam, and the remainder of the fundamental beam was focused into a 1 cm quartz cell containing water, thereby generating a white light continuum from 350 to 1300 nm. For probe wavelengths between 400 and 1000 nm the required part of the white light continuum was selected by a variable interference filter with a bandwidth of $\Delta\lambda/\lambda \approx 0.02$. To generate wavelengths in the range from 340 to 450 nm, the white light continuum was frequency doubled in a 2 mm BBO crystal, and the required wavelength was selected by rotating the BBO crystal according to the phase-matching angle for that particular wavelength. A Glan-Thomson polarizer was used to attain a linear polarization of the probe light, while a $\lambda/2$ wave plate was used to rotate the polarization

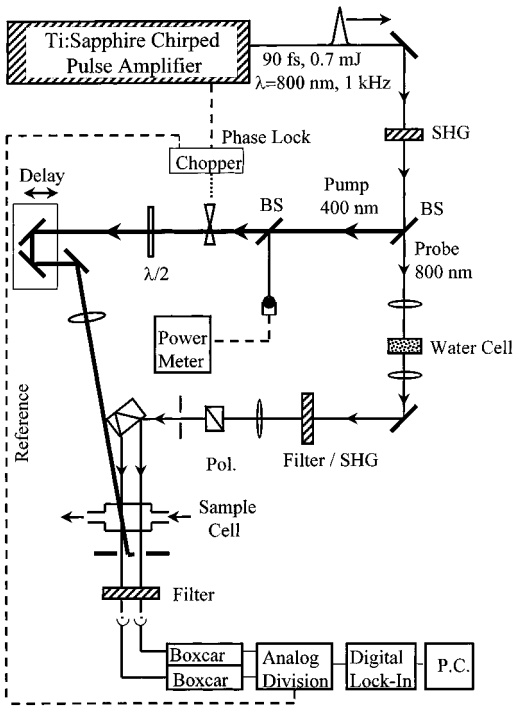

Figure 2. Experimental setup.

of the pump beam to 54.7° (magic angle) relative to that of the probe beam to remove contributions to the transient absorption from rotational reorientation of PNA. Before passing through the sample, the probe beam was divided into a signal and a reference beam by a 10 mm quartz window inserted at 45°. The pump beam was modulated at 0.5 kHz, phase-locked to the 1 kHz repetition rate of the regenerative amplifier, and made to cross the signal beam at an angle of ≈5°. The typical pump pulse energy was 150 μJ/pulse with a stability of better than ±2% over several hours, and the size of the pump beam was 4 mm ($1/e^2$) at the sample cuvette. The spot size of the signal beam was made much smaller than that of the pump beam to allow it to be situated well within the pump beam at the sample cell. After passing through the sample, the pump and the probe beams were spatially separated with iris diaphragms, and the probe beams were spectrally filtered by quartz dispersion prisms, before they were detected by two matched photodiodes and boxcar integrators. The ratio of the signal from the two boxcar integrators were sent to a digital lock-in amplifier referenced to the pump beam modulation.

Measurements taken on different days were put on the same absorption scale with an uncertainty of ±10% by making overlapping measurements. The reproducibility of the data was checked among consecutive scans as well as by repeating the experiment on different days using different samples. A series of experiments, in which the power of the pump pulse was changed by more than 1 order of magnitude, showed that the photoinduced changes of absorbance were proportional to the pump power. This indicates that two-photon absorption is insignificant. The measurements also showed that the photodynamics were independent of the pump power.

p-Nitroaniline (PNA), purity > 99%, was purchased from Fluka Chemika and used as received. The solvents used were HPLC grade 1,4-dioxane from Rathburn Chemicals and three times distilled water. The PNA solution was exchanged frequently during the series of measurements, and the flow through the 1 mm quartz cuvette was adjusted to ensure a fresh sample for each laser pulse. The optical density of the PNA solution was measured regularly with an uncertainty of <5%

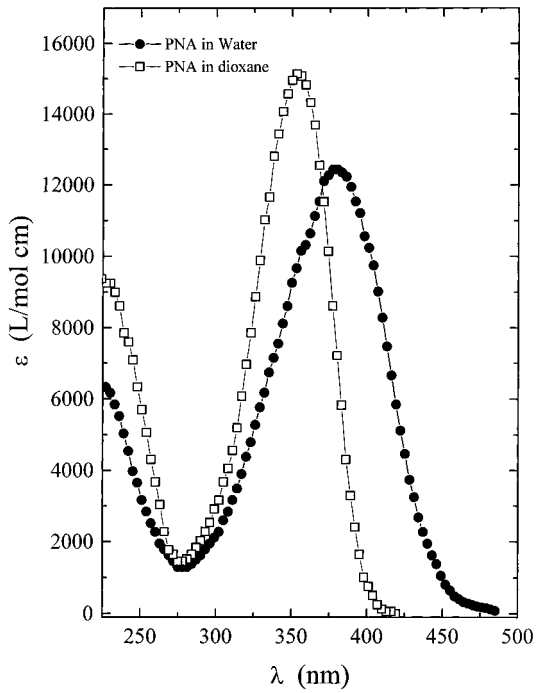

Figure 3. Steady-state charge-transfer absorption spectrum of PNA in water (●) and dioxane (□).

on a Cary 219 spectrophotometer, and the transient absorption spectra shown in section III have been corrected for the small variations in the concentration. After numerous measurements we found the overall reproducibility of the photoinduced changes in absorbance to be better than ±15%.

IV. Experimental Results

Static Absorption Spectrum. Figure 3 shows the charge-transfer absorption band of PNA in dioxane and water. The charge-transfer absorption band of PNA in water peaks at 380 nm and has a width of about 7200 cm^{-1} (fwhm), whereas that in dioxane is blue-shifted by 2000 cm^{-1} with a reduced width of 5000 cm^{-1}. The strong blue shift agrees with the notion that the excited state has a larger dipole moment than the ground state.

Description of Transient Data. In Figure 4 the transient absorbance, $\Delta A(\lambda,t)$, of PNA in (a) water and (b) dioxane produced by the 400 nm pump pulse is shown as function of the delay after the pump pulse in steps of 0.1 ps. The transient absorption spectra were obtained in steps of 1000 cm^{-1} in the spectral range from 29 400 cm^{-1} (340 nm) to 10 400 cm^{-1} (960 nm) and can be brought on a common absorption scale with an accuracy of ±15%, permitting an accurate determination of the temporal evolution of the absorption spectrum.

A representative selection of these measurements is shown in Figure 5. Common to many of the curves is an initial sharp dip resembling closely that obtained at the same wavelength when pure solvent is substituted for PNA without changing the alignment of the setup. Hence, we ascribe this peak to the two-beam coupling associated with the solvent, and take the temporal position of the peak to mark the point of zero delay ($t = 0$).

PNA in Water. At wavelengths shorter than 410 nm the transient absorption signal exhibits a strong initial absorption bleaching reflecting that pump-induced ground-state depletion dominates the observed dynamics. The ground-state absorption recovers within the first 2 ps, leaving a residual absorption bleaching of 5% of the initial value. Between 380 and 410 nm, the absorption recovery "overshoots" before returning to

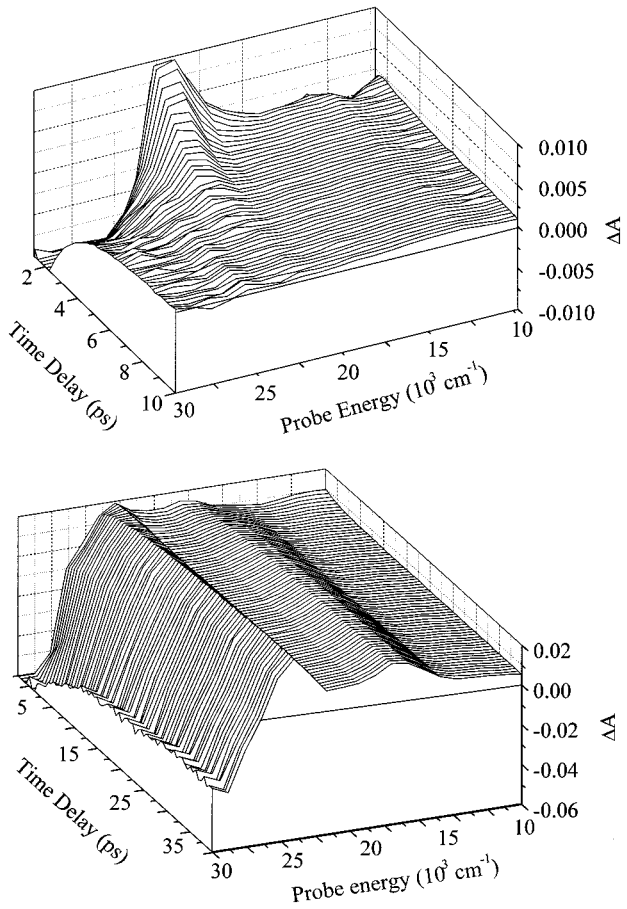

Figure 4. Transient absorption spectrum in the spectral range from 29 400 cm^{-1} (340 nm) to 10 400 cm^{-1} (960 nm) of PNA in (a, top) water and (b, bottom) dioxane produced by the 400 nm pump pulse. The transient ΔA spectra were obtained for every 0.1 ps and brought on a common absorption scale with an accuracy of ±15%, permitting an accurate determination of the temporal evolution of the absorption spectrum.

an almost zero level, indicating the presence of more than one absorbing component. The absorption of these secondary components relative to that of the ground state increases at longer wavelengths, resulting in a decreasing absorption recovery time from 1.8 ps at 340 nm to 0.5 ps at 380 nm. From 428 to 960 nm the initial instrument limited rise of the induced absorption is followed by a decay to a positive level, which remains constant for more than 100 ps. The residual induced absorption can be observed at all probe wavelengths but has a maximum at 700 nm.

PNA in Dioxane. The transient absorption of PNA in dioxane is very different from that of PNA in water. For probe wavelength within the CT band, the pump pulse induces a strong bleaching, due to the removal of ground-state PNA molecules. At 340 nm this absorption bleaching recovers on a time scale of 7±1 ps, approaching a constant level corresponding to 40 ± 5% of the maximum bleaching at short time delays. The residual bleaching lasts for more than 100 ps and is clearly larger than that in water. As the probe wavelength is tuned toward longer wavelengths, the bleaching is gradually replaced by a very large induced absorption. From 400 to 960 nm the transient absorption shows an instrument limited rise, which reaches a constant level after about 20 ps. As in the case of PNA in water, this constant absorption of PNA in dioxane is observed at all probe wavelengths but has two distinct absorption maxima at 550 and 410 nm.

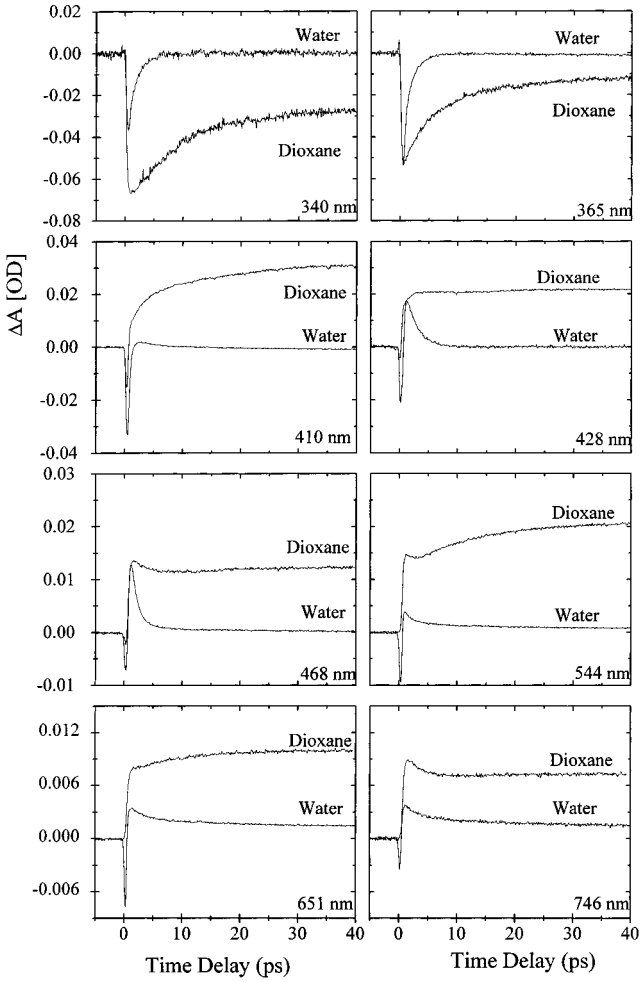

Figure 5. A representative selection of experimental pump−probe signals of PNA in water and dioxane.

V. Discussion

Interpretation of the Long Delay Transient Signal. The persistence of the induced absorption at visible probe wavelengths in Figures 4 and 5, combined with the fact that the ground-state absorption, observed at blue and UV wavelengths, does not fully recover, indicates that new long-lived states have been formed as a result of the photolysis. The strong phosphorescence observed in low-temperature rigid matrixes[28] and the rapid, radiationless decay of the S_1 state have partly been ascribed to a very rapid intersystem crossing to the triplet manifold.[18] In the case of PNA dissolved in nonpolar solvents it has even been suggested that the quantum yield for triplet-state formation is close to unity.[18] On the basis of these results, we suggest that a fraction of the photoexcited PNA molecules end up in a long-lived triplet state via fast intersystem crossing, from where two strong triplet−triplet transitions gives rise to the absorption spectrum observed in the visible and near-infrared (see Figure 4).

Intersystem Crossing Quantum Yield in Dioxane. To calculate the intersystem crossing yield, we assume that the permanent bleaching is solely due to intersystem crossing to the triplet state and that the triplet-state absorption is insignificant at 340 nm. If we, in addition, assume that the extinction coefficient of the excited singlet S_1 state is significantly smaller than the ground-state absorption, a lower value of the intersystem crossing yield can be estimated. Thus, taking the residual change in absorbance at 340 nm ($\Delta A(40\text{ ps}) = -0.026$) to indicate the concentration in the triplet state and the maximum bleaching ($\Delta A(0) = -0.065$) to indicate the initial concentration of excited PNA, the lower limit of the intersystem crossing quantum yield in dioxane is estimated to $\Phi_{ISC} \geq 0.40 \pm 0.05$. This result is in good agreement with the intersystem crossing quantum yield of $\Phi_{ISC} \approx 0.5$ of PNA in dioxane estimated by Schuddeboom et al.[18]

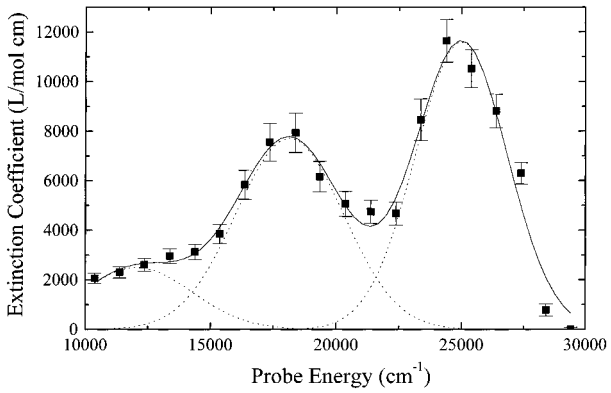

Figure 6. Triplet−triplet absorption spectrum of PNA in dioxane. To obtain the spectrum, we have taken the measured induced absorption at long delays and at each probe wavelength added the ground-state absorption contribution derived from the residual bleaching at 340 nm, scaled with the relevant absorption coefficient, given in Figure 1. Details are found in the text.

TABLE 1: Comparison of the Oscillator Strengths for the $T_1(^3A_1) \rightarrow T_9(^3A_1)$ and $T_1(^3A_1) \rightarrow T_8(^3A_1)$ Transitions Obtained from Our Experiment and from Calculation

measured values		calculated values[a]		
abs max (cm^{-1})	oscillator strength	abs max (cm^{-1})	oscillator strength	$T_n \leftarrow T_1$ excitations
25 000	0.23	25 000	0.10	$8\,^3A_1(\pi\pi^*) \leftarrow 1\,^3A_1(\pi\pi^*)$
18 000	0.17	16 000	0.085	$9\,^3A_1(\pi\pi^*) \leftarrow 1\,^3A_1(\pi\pi^*)$

[a]Reference 18.

Triplet−Triplet Absorption Spectrum in Dioxane. Following the intersystem crossing and relaxation, the transient spectra of PNA in dioxane shown in Figure 4b converge to two, perhaps three, absorption bands after 40 ps. The following analysis of the triplet−triplet transition is based on the absorption spectrum observed after 40 ps and the intersystem crossing quantum yield of 40 ± 5%. To extract the triplet−triplet absorption spectrum, we correct the induced absorption spectrum of Figure 4b for the ground-state absorption contribution, using the extinction coefficients of ground-state PNA, shown in Figure 3. The resulting triplet−triplet absorption spectrum depicted in Figure 6 shows two clear absorption bands centered at 25 000 and 18 000 cm^{-1}. The absorption maximum at 25 000 cm^{-1} is in good agreement with the position of the $T_1(^3A_1) \rightarrow T_9(^3A_1)$ transition predicted by Bigelow et al.,[17] while the absorption maximum at 18 000 cm^{-1} is assigned to the only other visible transition, $T_1(^3A_1) \rightarrow T_8(^3A_1)$, however shifted to higher energy (see Table 1). The oscillator strengths, *f*, derived from the experimental data are calculated using the equation[29]

$$f = (4.319 \times 10^{-9}\ \mathrm{L^{-1}\ mol\ cm^2}) \int \epsilon(\tilde{\nu})\, \mathrm{d}\tilde{\nu} \qquad (1)$$

where $\epsilon(\tilde{\nu})$ denotes the extinction coefficient, and the absorption bands have been approximated with Gaussian profiles as illustrated in Figure 6. The resulting oscillator strengths of $f = 0.23$ and $f = 0.17$ differ by only a factor of 2 from those predicted by Bigelow et al.[17] (see Table 1). The predicted oscillator strength[17] of any other calculated triplet−triplet transition between 300 and 1000 nm is several orders of

magnitude smaller than the experimentally observed. The oscillator strength is calculated assuming the lower intersystem crossing quantum yield of 40%, but using a higher quantum yield changes the oscillator strength by less than 1 order of magnitude and does thus not severely change the agreement with the calculated values. The small additional absorption band at 12 000 cm^{-1} cannot, on the other hand, be ascribed to any specific transition when compared with the calculated spectrum by Bigelow et al.[17] Great caution must, however, be exercised when comparing experimental data from one molecule with low-level ab initio calculations. Considering the lack of agreement between the different theoretical calculations, the agreement between theory and experiment for both the position and strength of the triplet−triplet transitions might still be accidental.

Intersystem Crossing Quantum Yield in Water. Since the dipole moments of the excited triplet states are expected to be larger than that of the lower $T_1(^3A_1)$ state, stabilization is expected to red-shift the triplet absorption band in water relative to that in dioxane. Due to the biradical character of excited PNA, we expect the S_1-T_1 splitting to be very small. Thus, solvent-induced shifts in the triplet manifold are easily of the same magnitude as the solvatochromatic shift observed in Figure 3. Hence, the contribution from the triplet−triplet transition to the absorption at 340 nm is expected to be insignificant in water. Taking the residual bleaching at 340 nm ($\Delta A(40\text{ ps}) = -0.0011$) to indicate the concentration in the triplet state and the maximum change in absorbance ($\Delta A(0) = -0.037$) to indicate the initial concentration of excited PNA, the intersystem crossing quantum yield in water is estimated to be $\Phi_{ISC} = 0.03 \pm 0.02$. The much reduced quantum efficiency in water leads to a very small residual absorption at long delays, which we tentatively ascribe to triplet−triplet transitions centered around 700 nm. However, the quality of these data hardly warrants a spectral analysis similar to the one performed for dioxane. Before considering the decrease in intersystem crossing efficiency in detail, the kinetics of the intersystem crossing will be presented below.

Kinetic Model and Intersystem Crossing Rates in Water and Dioxane. Although the details of the relaxation of the initially excited PNA molecules may be more complex, we represent the transient absorption in terms of the simplest possible kinetic scheme described in Figure 1, assuming that the initially excited singlet state S_1 decays with the rate K_{ISC} to T_1 and the rate K_{IC} to the ground state, S_0. This simplified description leads to the following equation for the intersystem crossing quantum yield

$$\Phi_{ISC} = K_{ISC}/(K_{ISC} + K_{IC}) \tag{2}$$

where the denominator of eq 2 is given by

$$K_{ISC} + K_{IC} = \frac{1}{\tau_{ISC}} + \frac{1}{\tau_{IC}} = \frac{1}{\tau_{S_1}} \tag{3}$$

According to this model, the instrument-limited rise time of the triplet absorption signal in Figure 5 implies that the lifetime of the excited singlet state is less than 0.3 ps. From the above equations the time constant for triplet formation can be evaluated using the estimated intersystem crossing quantum yield in water and dioxane of 0.03 and 0.4, respectively:

$$\tau_{ISC} = \frac{1}{K_{ISC}} = \frac{\tau_{S_1}}{\Phi_{ISC}} \leq \frac{0.3\text{ ps}}{\Phi_{ISC}} \tag{4}$$

The result is an intersystem crossing time $\tau_{ISC} \leq 10$ ps in water and $\tau_{ISC} \leq 0.8$ ps in dioxane, while the time constant for internal conversion is $\tau_{IC} \leq 0.3$ ps in water and $\tau_{IC} \leq 0.5$ ps in dioxane. The rate constants are listed in Table 2. The very fast intersystem crossing of PNA in dioxane suggests that the S_1 and T_1 states are nearly degenerate and hence causes a substantial mixing between the singlet and triplet system. When going to polar solvents, the intersystem crossing yield is reduced by almost an order of magnitude. In general, two effects can cause the reduced yield: either a solvent-dependent internal conversion rate or a solvent-dependent singlet−triplet mixing. When going from water to dioxane, we see indications that the internal conversion rate drops by a factor of 2 ($\tau_{IC} \leq 0.3$ ps in water and $\tau_{IC} \leq 0.5$ ps in dioxane). For a solvent-mediated internal conversion process it is not surprising that the rate is higher in polar water compared to nonpolar dioxane. So at least part of the increased triplet yield in dioxane is caused by a reduced internal conversion rate. Several effects can contribute to a solvent-dependent singlet−triplet coupling. Both the S_1 and T_1 states have strong CT($\pi\pi^*$) character, resulting in a large solvatochromatic shift. In polar solvents the ^{3}CT($\pi\pi^*$) states will thus shift well below states with ^{3}(nπ^*) character. This will reduce the singlet−triplet mixing according to El-Sayed's rule, as the mixing is dominated by $^1(\pi\pi^*)-^3(\pi\pi^*)$ interactions. In nonpolar solvents, however, the splitting between the ^{3}CT-($\pi\pi^*$) state and the ^{3}(nπ^*) states is reduced, and the singlet−triplet mixing is enhanced due to the larger proportion of $^1(\pi\pi^*)-^3(n\pi^*)$ interactions. A similar switching of states, dependent on solvent polarity, was recently observed in 4-aminobenzophenone.[30] If, on the other hand, the dipole moments of the singlet and triplet CT state differ substantially, as suggested in ref 17, then the two states will experience a different shift upon solvation in a polar solvent. Consequently, the near degeneracy is lifted in polar solvents, thereby reducing the singlet−triplet mixing. The possibility of twisted triplet states (the singlet states are not twisted[25]) could also be taken into account when considering a solvent-dependent singlet−triplet crossing. Twisting of the nitro group upon excitation will influence the singlet−triplet crossing, and if the twisting takes place, it is likely to depend on the surrounding solvent. However, a more detailed study of the initial intramolecular dynamics responsible for the observed yields will require both theoretical investigations of the singlet−triplet mixing and experimental investigations with shorter optical pulses than those used in the present work.

TABLE 2: Estimated Intersystem Crossing and Internal Conversions Times for PNA in Dioxane and Water, Calculated Using the Estimated Intersystem Crossing Quantum Yield

solvent	τ_{ISC} (ps)	τ_{IC} (ps)	Φ_{ISC}
water	10.0	0.3	0.03 ± 0.02
dioxane	0.8	0.5	0.40 ± 0.05 ($\approx$0.5)[a]

[a] Suggested intersystem crossing quantum yield for PNA in dioxane (ref 18).

Interpretation of the Time Evolution of the Transient Absorption Signal. *Water*. The transient absorption spectra of PNA in water, depicted in Figure 4a, exhibit a strong initial absorption from 400 to 590 nm (24 000−17 000 cm^{-1}) centered at 450 nm. The absorption maximum moves toward the absorption maximum of equilibrated PNA at 380 nm (26 000 cm^{-1}) (Figure 4) as it decays on a 2 ps time scale. Simultaneously, the induced bleaching of the absorption caused by the removal of ground-state PNA recovers on a similar time scale. Since the dipole moment of the excited singlet state is much bigger than that of the ground state, the internal conversion

$S_1 \rightarrow S_0$ is accompanied by a big change in the dipole moment, leaving the surrounding water molecules nonequilibrated with respect to the new charge distribution. The subsequent reorientation of the solvent molecules may result in an appreciable transient spectral shift, which for water is believed to decay within 0.5 ps.[31] However, the observed temporal evolution of the transient absorption is significantly slower than the solvation dynamics of water and thus cannot solely be ascribed to solvent reorganization. In addition to solvent reorganization, the transient absorption signal may have a large contribution from energy relaxation in the electronic ground state. Fast internal conversion in the singlet system leads to a rapid population of the excited vibrational states of the electronic ground state. This excess energy is dissipated into the solvent either via vibrational relaxation of the initially excited vibrational mode or by energy redistribution to other vibrational modes. In either case the absorption spectra of the vibrationally excited states likely have an absorption spectrum different from that of the vibrational ground state. The temporal evolution of the absorption spectrum combined with the fact that the induced absorption relaxes on a time scale comparable to the 1.8 ± 0.3 ps recovery time of the ground-state absorption strongly indicates that energy relaxation to the vibrational ground state following internal conversion is the dominant cause for the transient absorption observed in Figure 4.

Dioxane. A spectral evolution of the ground-state absorption similar to that of PNA in water is not observed in dioxane, because the efficient intersystem crossing results in a reduced internal conversion. Moreover, the strong triplet−triplet absorption of PNA in dioxane dominates the spectral region, where the absorption associated with the vibrationally excited singlet state is expected to appear. Hence, the origin of the spectral evolution observed at short delays from 340 to 500 nm (Figure 4 b) may arise from a combination of solvent reorganization and energy relaxation in both the triplet state and the ground state, but due to the strong triplet−triplet absorption, the data hardly warrant a more detailed analysis of the relaxation dynamics.

The different photophysical behaviors of PNA in water and dioxane are also clearly observed, when comparing the final energy relaxation times in the two solvents. Taking the recovery time of the ground-state absorption to reflect the time scale for internal conversion to the ground state and subsequent energy relaxation to the vibrational ground state gives an energy relaxation time of PNA in dioxane of 7 ± 1 ps and 1.8 ± 0.3 ps in water. The much faster vibrational relaxation of PNA in water thus agrees with the notion of a stronger interacting between the strong dipole and the polar solvent.[32,33]

VI. Summary

The ultrafast photophysics of PNA in water and dioxane has been studied using femtosecond transient absorption spectroscopy. PNA was photoexcited at 400 nm and probed in the spectral range from 340 to 960 nm. The data reveal that relaxation in the excited singlet state, intersystem crossing to the triplet state, and internal conversion to the electronic ground state take place within a few hundred femtoseconds. The subsequent relaxation in the electronic ground state occurs on a time scale of 1.8 ± 0.3 ps in water and 7 ± 1 ps in dioxane, while the triplet-state lifetime is >1 ns in both solvents. The intersystem crossing quantum yield is determined to be $\Phi_{ISC} = 0.03 \pm 0.02$ in water and $\Phi_{ISC} \geq 0.40 \pm 0.05$ in dioxane. On the basis of the quantum yields for triplet formation, we estimate the time constants for intersystem crossing and internal conversion to be $\tau_{ISC} \leq 10$ ps and $\tau_{IC} \leq 0.3$ ps in water and $\tau_{ISC} \leq 0.8$ ps and $\tau_{IC} \leq 0.5$ ps in dioxane. The fast intersystem crossing of PNA in dioxane indicates a substantial mixing of the S_1 and T_1 states that are nearly degenerate. Accordingly, the order of magnitude decrease in the intersystem crossing yield when going from dioxane to water is ascribed to a solvent-induced increase in internal conversion rate as well as a lowering of the coupling between the S_1 and T_1 states. Two triplet−triplet absorption bands in dioxane were identified at 18 000 and 25 000 cm^{-1}, in agreement with previous theoretical calculations.

Acknowledgment. This work was financially supported by the Carlsberg Foundation and the SNF-Center for Molecular Reaction Dynamics and Laser Chemistry. The authors thank K. V. Mikkelsen, K. Sylvester-Hvid, and S. Uttrup-Pedersen for stimulating discussions.

References and Notes

(1) Mikkelsen, K. V.; Kmit, M. *Theor. Chim. Acta* **1995**, *90*, 307.
(2) Mikkelsen, K. V.; Luo,Y.; Ågren, H.; Jørgensen, P. *Chem. Phys. Lett.* **1993**, *207*, 190.
(3) Luo, Y.; Ågren, H.; Vahtras, O.; Jørgensen, P. *J. Chem. Phys.* **1994**, *100*, 8240.
(4) Ågren, H.; Vahtras, O.; Koch, H.; Jørgensen, P. Helgaker, T. *J. Chem. Phys.* **1993**, *98*, 6417.
(5) Willetts, A.; Rice, J. E.; Burland, D. M.; Shelton, D. P. *J. Chem. Phys.* **1992**, *97*, 7590.
(6) Wortmann, R.; Krämer, P.; Glania, C.; Lebus, S.; Detzer, N. *Chem. Phys.* **1993**, *173*, 99.
(7) Daniel, C.; Dupuis, M. *Chem. Phys. Lett.* **1990**, *171*, 209.
(8) Sim, F.; Chin, S.; Dupuis, M.; Rice, J. E. *J. Phys. Chem.* **1993**, *97*, 1158.
(9) Morrell, J. A.; Albrecht, A. C. *Chem. Phys. Lett.* **1979**, *64*, 46.
(10) Maslianitsin, I. A.; Shigorin, V. D.; Shipulo, G. P. *Chem. Phys. Lett.* **1992**, *194*, 355.
(11) Karna, S. P.; Prasad, P. N.; Dupuis, M. *J. Chem. Phys.* **1991**, *94*, 1171.
(12) Stähelin, M.; Burland, D. M.; Rice, J. E. *Chem. Phys. Lett.* **1992**, *191*, 245.
(13) Teng, C. C.; Garito, A. F. *Phys. Rev. B* **1983**, *28*, 6766.
(14) Hiberty, P. C.; Ohanessian, G. *J. Am. Chem. Soc.* **1984**, *106*, 6963.
(15) Sinha, H. K.; Yates, K. *J. Am. Chem. Soc.* **1991**, *113*, 6062.
(16) Malar, E. J. P.; Jug, K. *J. Phys. Chem.* **1985**, *89*, 5235.
(17) Bigelow, R. W.; Freund, H. J.; Dick, B. *Theor. Chim. Acta* **1986**, *63*, 177.
(18) Schuddeboom, W.; Warman, J. M.; Biemans, H. A. M.; Mejler, E. W. *J. Phys. Chem.* **1996**, *100*, 12369.
(19) Wolleben, J.; Testra, A. C. *J. Phys. Chem.* **1977**, *81*, 429.
(20) Bertinelli, F.; Palmieri, P.; Brillante, A. Taliani, C. *Chem. Phys.* **1977**, *25*, 333.
(21) Ledger, M. B.; Suppan, P. *Spectrochim. Acta* **1967**, *23A*, 641.
(22) Carsey, T. P.; Findley, G. L.; McGlynn, S. P. *J. Am. Chem. Soc.* **1979**, *101*, 4502.
(23) McGlynn, S. P.; Azumi, T.; Kinoshita, M. *The Triplet State*; Prentice-Hall: Englewood Cliffs, NJ, 1969.
(24) Woodford, J. N.; Pauley, M. A.; Wang, C. H. *J. Phys. Chem. A* **1997**, *101*, 1989.
(25) Sinha, H. K.; Yates, K. *Can. J. Chem.* **1991**, *69*, 550.
(26) Mohanalingam, K.; Hamaguchi, H. *Chem. Lett.* **1997**, 157.
(27) Mohanalingam, K.; Hamaguchi, H. *Chem. Lett.* **1997**, 537.
(28) Khalil, O. S.; Seliskar, C. J.; McGlynn, S. P. *J. Chem. Phys.* **1973**, *58*, 1607.
(29) Gilbert, A.; Baggott, J. *Essentials of Molecular Photochemistry*; Blackwell Scientific Publications: Oxford, 1991.
(30) Ghoneim, N.; Monbelli, A.; Pilloud, D.; Suppan, P. *J. Photochem. Photobiol. A: Chem.* **1996**, *94*, 145
(31) Jimenez, R.; Fleming, G. R.; Kumar, P. V.; Maroncelli, M. *Nature* **1994**, *369*. 471.
(32) Whitnell, R. M.; Wilson, K. R.; Hynes, J. T. *J. Chem. Phys.* **1992**, *96*, 5354.
(33) Cho, M. *J. Chem. Phys.* **1996**, *106*, 10755.